Clim Dyn
DOI 10.1007/s00382-016-3098-3

The spring relationship between the Pacific-North American pattern and the North Atlantic Oscillation

Nicholas Soulard[1] · **Hai Lin**[2]

Received: 7 October 2015 / Accepted: 19 March 2016

Abstract The Pacific-North American pattern (PNA) and North Atlantic Oscillation (NAO) are two dominant modes of low-frequency variability in the Northern Hemisphere winter. Generally these two patterns are separable and uncorrelated in both space and time. However, dating back to the 1970s there have been studies which have linked the Aleutian and Icelandic low intensities, and shown that a significant temporal correlation does, on occasion, occur. Each of these semi-permanent low pressure systems is a part of the PNA and NAO patterns, respectively, and therefore, given a link between the two semi-permanent low pressure systems, we explore whether a link between the PNA and NAO also appears. Recently studies have found such a link during the winters of certain decades. The present study, documents an observed relationship between the PNA and NAO which is consistently present during the spring and early summer. This relationship is shown to be due to the fact that the PNA and NAO are spatially overlapping projections of the same pattern of variability, given by the first EOF of 500 hPa geopotential height. Both the PNA and NAO patterns correlate more strongly to the first EOF's spatial pattern, resembling the Aleutian low-Icelandic low seesaw pattern, than the rotated EOF (REOF) loading patterns used to compute their respective indices. Furthermore, when the two patterns are correlated, the effect of El-Nino on the Northern Hemisphere is separate from the pattern associated with the PNA. Finally, we examine a 21-year period in the winter for which the PNA and NAO are significantly correlated, and find that the conclusions drawn from the spring hold true. The results presented herein demonstrate that defining the PNA and NAO based upon typical loading patterns may not be the ideal approach; especially given that the patterns are spatially similar and covary in time.

Keywords PNA · NAO · Seasonal climate · Climate variability

1 Introduction

The North Atlantic Oscillation (NAO) is a fundamental mode of internal variability which explains a large proportion of atmospheric variance in all seasons of the year (Hurrell et al. 2003; Barnston and Livezey 1987). It consists of an oscillation in pressure between Iceland and the subtropical Atlantic Ocean, and impacts the location of the Atlantic Jet, and thus the weather over much of Europe (Hurrell and van Loon 1997). Still a subject of debate within the community is whether the NAO is simply a regional manifestation of the Arctic Oscillation (AO) (Wallace 2000). The present study is not concerned with whether or not the NAO and AO are distinct, but rather we will refer to the AO when we wish to distinguish between a hemispheric and a regional scale pattern.

The Pacific-North American pattern (PNA), another important mode of low-frequency variability, consists of a wave train emanating from the tropical Pacific and arching towards Florida (e.g. Wallace and Gutzler 1981). The PNA has a well-documented link to El-Nino related sea-surface

✉ Nicholas Soulard
nicholas.soulard@mail.mcgill.ca

Hai Lin
hai.lin@ec.gc.ca

[1] Department of Atmospheric and Oceanic Sciences, McGill University, Montreal, QC, Canada

[2] Atmospheric Numerical Weather Prediction Research, Environment Canada, Dorval, QC, Canada

Published online: 28 March 2016

temperature (SST) variations and thus its phase tends to be partially predictable due to the fairly good predictability of the tropical Pacific SST (Horel 1981, Mo et al. 1998; Latif et al. 1994). There have been studies indicating that the PNA, while being a forced mode of variability, also appears as an internal mode (e.g. Straus and Shukla 2002). There has also been some debate as to whether the ENSO-forced Northern Hemisphere pressure variability is synonymous with the PNA. Most studies speak of the ENSO-forced variability generating a PNA-like pattern, and the PNA (as an internal mode of variability) interchangeably; however, some studies have pointed out that the two are not necessarily the same (Straus and Shukla 2000, 2002). It may therefore be possible to distinguish between the forced PNA-like mode and the PNA internal mode if the Northern Hemisphere geopotential height field loses its synchrony with the tropical Pacific SST variability.

Here it is helpful to note that while ENSO SST anomalies can provide a forcing on the Northern Hemisphere geopotential height field and generate a response (hence external forcing), this response has a linear and non-linear components (e.g. Hoerling et al. 2001; Peng and Kumar 2005; Straus and Shukla 2002). However, as discussed in Lin and Derome (2004) the linear component is dominant. It is likely that the PNA is fundamentally an internal mode of variability, present during all phases of ENSO, but whose variability is modulated by tropical forcing (Johnson and Feldstein 2010). Furthermore, the NAO also exhibits some non-linearity with regards to tropical Pacific forcing; this response is small compared to that of the PNA (Pozo-Vázquez et al. 2001, 2005; Lin and Derome 2004).

Both the PNA and NAO reach their maximum amplitude in the winter months; however, unlike the NAO, the PNA is prominent mainly during the Northern Hemisphere cold season (Barnston and Livezey 1987). Given that both teleconnection patterns are strongest, and most prominent during the winter months, their loading patterns and the stations used to define the various forms of the PNA and NAO indices, are all closely related to these winter patterns (e.g. Wallace and Gutzler 1981; Barnston and Livezey 1987; Horel 1981). Using these patterns and stations to define teleconnection indices assumes a certain amount of season-to-season and year-to-year stationarity in the teleconnection patterns.

Given that the PNA and NAO are defined as regional patterns, their archetypal patterns do not project onto one another, and in general there is little correlation between the two time series of these teleconnection patterns during the winter. The PNA and NAO are each associated with one of the semi-permanent centres of variability located over the Aleutian Islands and Iceland, respectively (Blackmon et al. 1984). These two centres of variability do not always vary independently, but are at times anti-correlated which suggests a possible link between the PNA and NAO (van Loon and Rogers 1978; Honda et al. 2001). Song et al. (2009) examined the day-to-day variability between the PNA and NAO. They found that the two patterns are linked through waves emanating from the Pacific and breaking over the Atlantic sector, thus linking the Pacific and Atlantic storm tracks, and hence the PNA and NAO. While these transient effects likely play a role in the interannual variability, the main focus of this study is on the low-frequency forcing from the tropical Pacific. Honda et al. (2001) found a strong anti-correlation (-0.70) between the Aleutian low and Icelandic low intensities during the late winter and early spring for the time period of 1979–1994. However when looking at the entire currently available dataset we find that the correlation between the winter PNA and NAO indices is insignificant during the winter (correlation of -0.07), yet slightly higher (although still statistically insignificant) for the later winter months examined by Honda et al. (2001). There have since been studies which have shown that the existence of a link between the NAO and the PNA during the winter months is variable and depends on the sub-period of data examined (e.g. Pinto et al. 2010). This suggests that the varying times for which various studies have documented links between either the Aleutian and Icelandic lows, or the PNA and NAO, may simply be due to a temporal oscillation of their link.

This study will examine the relationship between these two teleconnection patterns on a seasonal time-scale over all three-month seasons of the year. The teleconnection indices are derived by projection of the geopotential height anomalies of the target season onto the REOF-derived loading patterns for each of the teleconnection patterns. The REOF analysis is performed on monthly mean anomalies for all months in the years of 1948–2004, as in Lin et al. (2009). Since the REOF analysis makes use of all months, the patterns derived in this way are valid for all months of the year; however, more weight will be given to the winter months since atmospheric variability is greater at this time. The associated teleconnection patterns for the target season are then defined as the regression of the seasonal teleconnection indices onto the geopotential height field of the target season. In this way, given the relative importance of each centre in the loading pattern, and its relationship to all other points, the structures of the teleconnection patterns may vary. Therefore considering the apparent connection between these two teleconnection patterns, one may question whether the associated patterns remain spatially orthogonal during the season in question. If not, then the validity of indices derived by projection onto typical loading patterns, and station based indices, may also be in question since the centres of variability highlighted in both methods may not be present at the time or simply associated with both teleconnection patterns. Each of these cases

would yield teleconnection patterns which do not resemble their typical configuration and/or resemble a sort of aggregate pattern, with features of both patterns present. Moreover, in either case, defining the responses of the teleconnections in other fields may yield somewhat deceptive results, insofar as forcing the teleconnection patterns' time series to vary with centres which may not be active, or even associated with the underlying mode of variability, will result in a spurious teleconnection time series.

This study will progress as follows: in section two the data and methodology used will be presented. The identification of a spring/early summer relationship will be discussed in section three. In section four the results of the regression and EOF analyses will be presented. Section five will consist of an example of a winter case. A summary and discussion of the results will conclude this paper in section six.

2 Data and methodology

The data used consists of 66 years of 500 hPa geopotential height (Z500), near-surface air temperature (T2 m), and sea-surface temperature (SST) from the National Centers for Environmental Protection/National Center for Atmospheric Research (NCEP/NCAR) reanalysis (Kalnay et al. 1996). The data lies on a 2.5° × 2.5° latitude-longitude grid spanning the years 1948–2013. We compute three-month-mean fields to put emphasis on the low-frequency variability and to partly filter out climate noise. We use three-month mean anomalies to examine the interannual relationship between the PNA and NAO patterns, and their associated time series. The analysis domain is limited to the Northern Hemisphere.

Temporal correlation is used to examine whether the phase and amplitude of two patterns covary, while pattern correlation is used to then compare the spatial fields associated with two time series. Since many points on the maps are not independent we assume 50 degrees of freedom (for a 504 point map), thus providing a very conservative estimate of the amount of independent points. Using both temporal and pattern correlations allows a more quantitative comparison to be made rather than just a subjective interpretation of patterns. Here 50 degrees of freedom are used based on the fact that in a given regression plot for either the PNA or NAO time series against the 500 hPa geopotential height field, centres of significant correlation tend to span at most 10 grid points. Hence for a conservative estimate of the number of independent points we assume that only one in ten grid points vary independently.

To extract dominant modes of variability which are active during a given time we use empirical orthogonal functions (EOFs). Their principal components allow some quantitative comparison to be made between the time-variance of the mode of interest against the teleconnection indices (defined below). We are then able to compare regressions of various fields onto the teleconnection indices against those associated with the principal components of the modes of variability to demonstrate the similarities and differences evident between them.

The archetypal NAO and PNA patterns are identified using rotated empirical orthogonal functions (REOFs) of monthly-mean anomalies for all months of 500 hPa geopotential height (Fig. 1), following Barnston and Livezey (1987). The REOFs are computed over the Northern Hemisphere between 20°N and 85°N and are on a 5° × 10° latitude-longitude grid. As stated above, the time and space variabilities are strongest during the winter months and therefore the associated REOF patterns are dominated by the winter season. The REOF patterns derived in this way are valid for all seasons throughout the years, and so the seasonal time indices are derived by projecting the 500 hPa

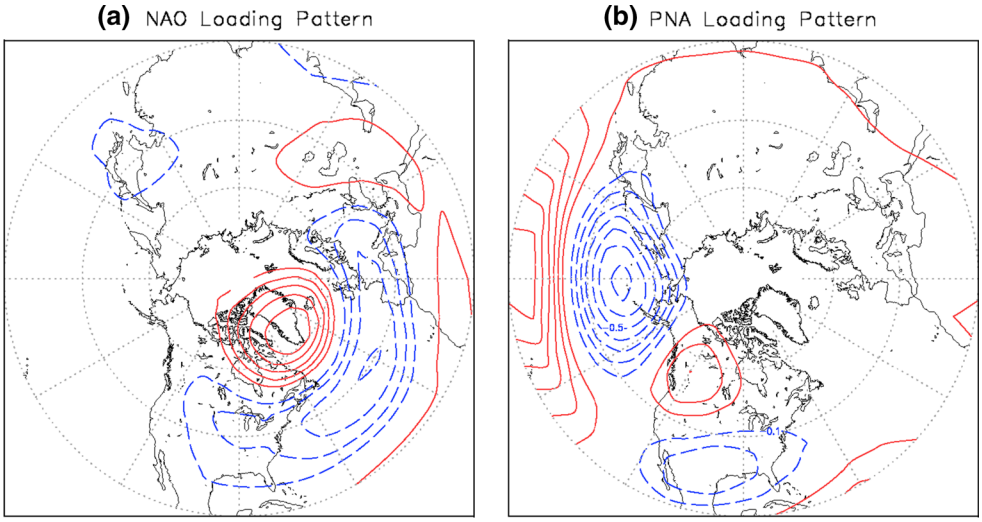

Fig. 1 The loading patterns for the **a** negative NAO, and **b** positive PNA teleconnection patterns

geopotential height anomalies from the target three-month season onto the REOF loading patterns. We subsequently regress the three-month-mean 500 hPa geopotential height anomalies of the target season onto these time series to obtain the PNA and NAO patterns at the desired time. Note that the REOF patterns are computed, and the same patterns are used as the loading patterns for all seasons. Furthermore, the resulting PNA and NAO patterns may differ from the structures of the REOF patterns above, as the latter were obtained using all months throughout the years of 1948–2004, while the former apply only to the target three-month "season" (three-month mean) for the years 1948–2013. Therefore the regression patterns may differ from the REOF loading patterns due to the different anomalies used in the two computations.

3 Spring correlation

The relationship between the PNA and NAO is examined using three-month-mean 500 hPa geopotential heights, staggered by a month (e.g. Dec-Feb, Jan-Mar, Feb-Apr, etc.). The PNA and NAO indices for each of these three-month seasons is derived in the manner described in the previous section. We simultaneously correlate the indices over a 65 year time series, 1949–2013 (where the year corresponds to that of the centre month in the three-month-mean) to determine how their interannual relationship varies from season to season (Fig. 2). There is statistically significant correlation (>95 % significance level) between the PNA and NAO indices from the FMA season through to MJJ with a maximum in AMJ. This extended period of correlation is not surprising given that the months used in the computation of the indices overlap with one another. The correlation between the PNA and NAO reaches −0.46 in AMJ and passes the 99 % significance threshold. During the remainder of the year there is no statistically significant correlation between the two patterns. Presented in Fig. 3 are the scatter plots of the NAO index against the PNA index for both the spring and winter. It is clear that during the winter months there is no relationship between the PNA and NAO indices. Conversely, in the spring there is an evident negative slope to the points, and this slope is significantly different from zero at the 95 % level. This relationship is consistent with the study carried out by Honda et al. (2001), which found a fairly high anti-correlation between the monthly Aleutian and Icelandic low intensities. The correlation between the PNA and NAO is slightly weaker and occurs later in the year. However, when examining the correlation for the Icelandic and Aleutian low intensities over the same regions, and over the same time period as described in Honda et al. 2001, we obtain similar results to theirs (not shown). The weaker, and later occurring correlation when using the entire available record can be explained by the presence of other centres used to compute the PNA and NAO indices, which may not perfectly covary with the Aleutian or Icelandic lows. The difference in timing between the present study and past studies may also imply a variable, non-stationary, relationship between the two patterns of variability (Pinto et al. 2010).

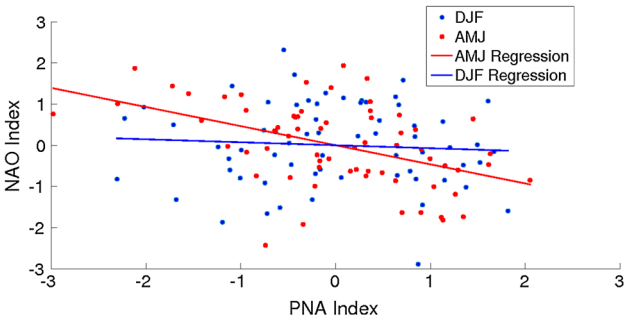

Fig. 3 *Scatter plot* of the NAO index versus the PNA index for the spring (April–June; *red*), and the winter (December–February; *blue*). The *lines* denotes the regression line for a linear relationship between the PNA and NAO indices for each of the two seasons

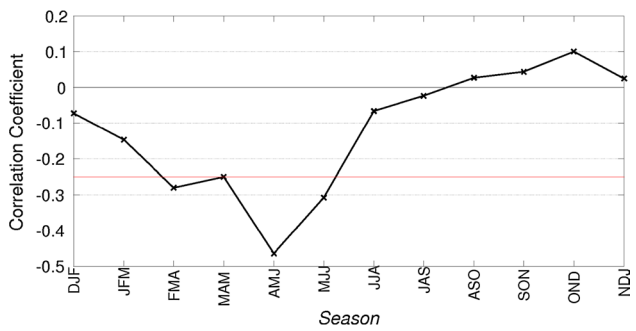

Fig. 2 Correlation between PNA and NAO indices for each three-month season. The 95 % significance level is indicated by the *red line*

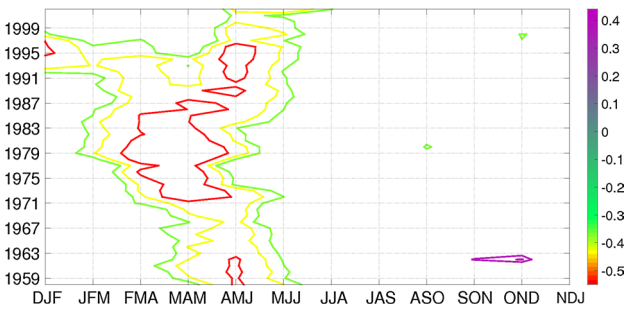

Fig. 4 21-year moving window correlation between PNA and NAO indices. Values passing the 90, 95, and 99 % significance levels are contoured in *green*, *yellow*, and *red*, respectively

Following Pinto et al. 2010, we computed a 21-year running correlation between the PNA and NAO indices (Fig. 4). It is clear that the correlation between the PNA and NAO is largely independent of the time period of data examined during the spring; however, we note an inter-decadal variation in the season where the two patterns are most significantly correlated. This variability explains the differing results of many studies which examine various subsections of the data and thus produce slightly dissimilar times for which the Aleutian and Icelandic low, or the PNA and NAO, are correlated (e.g. Pinto et al. 2010; Honda et al. 2001; Van Loon and Rogers 1978). Figure 4 provides a depiction of the inter-decadal variability of the relationship between the PNA and NAO for all three-month seasons. It also elucidates some smaller time-scale features, such as the winters of 1985–2005, where the PNA and NAO indices are significantly correlated.

The variable winter relationship between the PNA and NAO presented in Pinto et al. (2010) becomes apparent when examining the winters of 1985–2005. At this time a statistically significant correlation between the time series of the two patterns of −0.59 (surpassing the 99 % significance level) is observed. Zhao and Moore (2009) linked the correlation between the NAO and Aleutian pressure variations to the positive phase of the Pacific Decadal Oscillation (PDO) when the tropical Pacific SST has less influence on the Northern Hemisphere geopotential height field. A disconnect between the Northern Hemisphere geopotential heights and the tropical Pacific SST would allow internal dynamics to play a relatively larger role in the variability of the teleconnection patterns. We use the Nino-3.4 index as a metric for the variability of the tropical Pacific SST. During the winter season (DJF) we expect to see a relatively high correlation between the PNA and the Nino-3.4 index. This is indeed the case, the correlation between the two reaches 0.47 during the winter, which is significant to the 99 % level. Examining the spring, when the relationship between the PNA and NAO is strongest, we see that the correlation between the PNA and the Nino-3.4 index has dramatically decreased to 0.25 (barely passing the 95 % significance level). Moreover we would expect to see a PNA-like response in the Northern Hemisphere geopotential height field to the El-Nino SST variability. During the winter El-Nino's influence on the Northern Hemisphere geopotential height field is quite extensive, and resembles the PNA pattern (not shown). These areas surpassing the 95 % significance level cover 30.5 % of the Northern Hemisphere (north of 20°N). During the spring months, El-Nino SST variations appear to have a much less extensive influence on the Northern Hemisphere height field, with only 12.0 % of the Northern Hemisphere surpassing the 95 % significance threshold (Fig. 5).

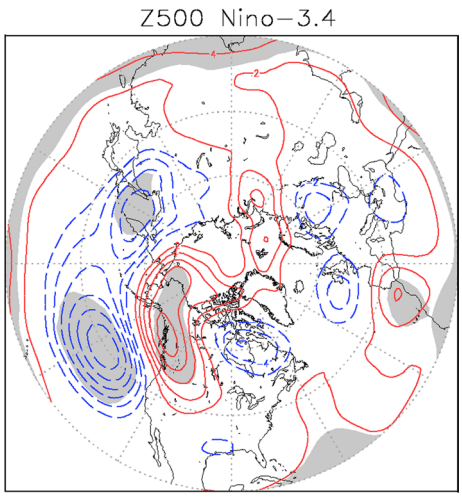

Fig. 5 Nino-3.4 index regressed onto the 500 hPa geopotential height field in AMJ. Contour interval is 2 m. The *grey shading* denotes areas passing the 95 % significance level

4 Results of the regression and EOF analyses

During the winter months the PNA and NAO are indeed two separate patterns. An EOF analysis of the winter 500 hPa geopotential height field demonstrates this fact (Fig. 6); the figures clearly show the first winter EOF as the NAO and the second as the PNA. This interpretation can be further cemented by examining the correlation between the principal components of these two modes with the teleconnection indices. Here the first principal component is strongly correlated with the NAO index, with a correlation coefficient of 0.93 (surpassing the 99 % significance level), while the second principal component correlates to the PNA index with a correlation coefficient of 0.89 (>99 % significance). This, coupled with the similarity between Figs. 1 and 6, shows that these two modes are indeed separate patterns of variability during the winter.

In the previous section we showed that there is a consistent correlation between the PNA and NAO indices during the spring and early summer months. Given this correlation we examine whether the two patterns remain separable in that season. Their respective spring regression patterns are presented in Fig. 7. The two patterns are similar, and reminiscent of the Arctic Oscillation (AO) in terms of the zonally symmetric structure (Thompson and Wallace 1998). The regression pattern associated with the NAO (Fig. 7a) regionally resembles the positive NAO, with a strong dipole between Greenland and the extratropical Atlantic Ocean. However, also present in the regression pattern are aspects normally associated with the negative phase of the PNA. There are two centres of variability in the Pacific: one over the tropics and another near the Aleutian Islands.

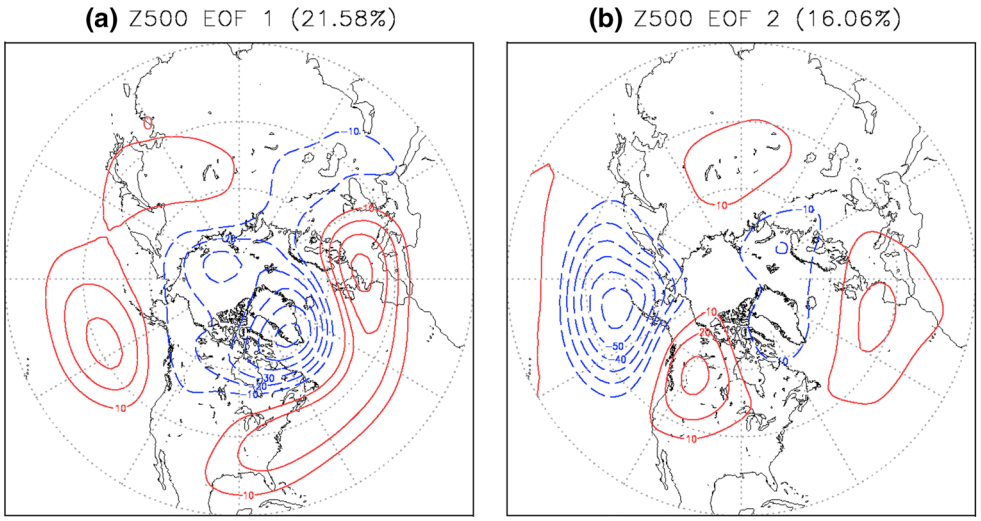

Fig. 6 The **a** first and **b** second EOF patterns for the DJF 500 hPa geopotential height field. The *bracketed values* show the amount of variance explained by each mode. Values correspond to a change of one standard deviation of the PC. Contour interval is 10 m

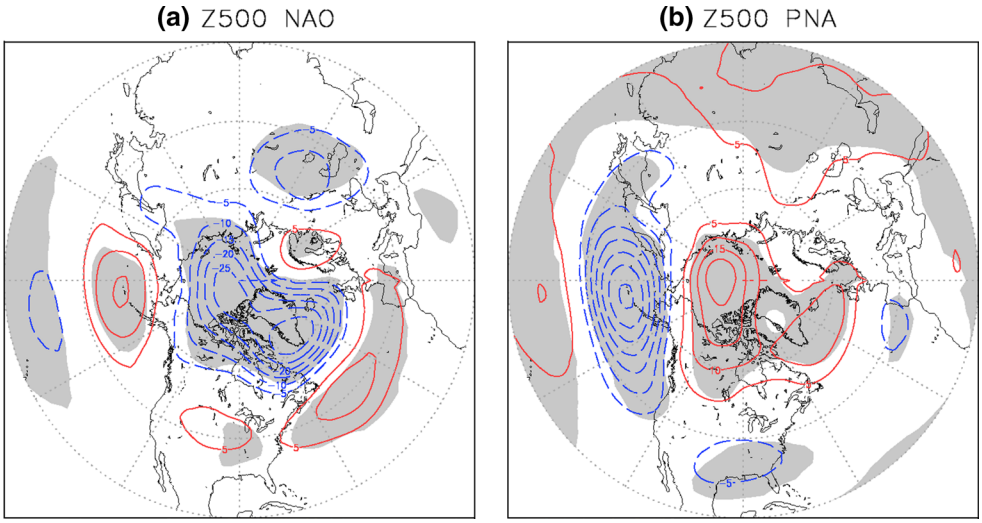

Fig. 7 Regression of AMJ **a** NAO, and **b** PNA index onto the 500 hPa geopotential height field. Contour interval is 5 m. *Grey shading* denote areas passing the 95 % significance level

Moreover, the centre covering the Arctic extends south into British Columbia. Likewise, the pattern associated with the positive PNA (Fig. 7b) has all of these same features (but of opposite sign), with the addition of the Florida pressure anomaly, and a weaker extratropical Atlantic centre. Their remarkable similarities lead to the question of whether the PNA and NAO are indeed two distinct, separable patterns in the spring during the period of analysis. An EOF analysis of the AMJ 500 hPa geopotential height field shows that the first EOF pattern resembles both the NAO and PNA regression patterns (Fig. 8a). Again this pattern bears resemblance to the zonally symmetric AO pattern. Although, however similar the first EOF is to the AO, its time series is still more strongly coupled to both the PNA and NAO than to the AO (Table 1). Both the PNA and NAO are strongly coupled to the first principal component, which explains more than a third of their respective variances. The similarity between the PNA, NAO, and the first EOF, coupled with the temporal relationship between the teleconnection patterns and the first principal component seems to indicate that the two patterns are not as distinct as often assumed.

To examine the structural similarities we use pattern correlation to facilitate a more quantitative measure of pattern similarity. Table 2 displays some such values over the Northern Hemisphere. The correlation in Table 2 is between patterns obtained by regressing the spring PNA and NAO indices onto the 500 hPa geopotential height fields, and the first two spring EOF patterns, as well as the REOF patterns used as the loading patterns to define the typical teleconnection patterns. Due to the large number of data points in the map (504 points) a correlation of 0.12 is sufficient to pass the 99 % significance threshold. With the reduced degrees of freedom to account for dependent points, this value increases to 0.37. During AMJ the spring patterns of the PNA and NAO significantly correlate with both the first and second EOF patterns (Fig. 8); however, the NAO is much more strongly related to the first EOF, while the PNA is equally related to both EOF patterns. In terms of

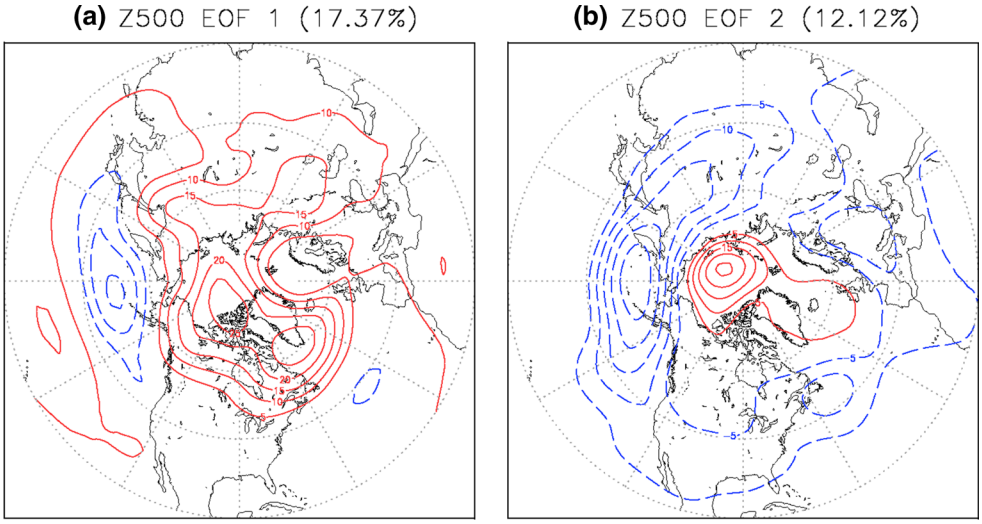

Fig. 8 First EOF of the AMJ 500 hPa geopotential height field. The variance explained by this mode is the *bracketed value*. Values correspond to a change of one standard deviation of the PC

Table 1 Temporal correlation between the AMJ PNA, NAO, and AO, and the first two PCs of 500 hPa geopotential height

AMJ	PC1	PC2
PNA	0.59	0.58
NAO	−0.70	−0.39
AO	0.40	**0.25**

The bold values denote 95 % significance, while underlined values denote 99 % significance

Table 2 Patterns correlation between the PNA and NAO AMJ regression patterns, and the loading patterns used to derive their indices, as well as the first and second EOF patterns

AMJ	Loading	EOF 1	EOF 2
PNA Regression	0.63	0.84	0.84
NAO Regression	−0.71	−0.92	−0.74

The bold values denote 95 % significance, while underlined values denote 99 % significance

the temporal correlation the same holds true (Table 1). In all cases, the pattern correlation between the regression patterns and the EOF patterns is higher than the correlation with the loading patterns used to derive the indices. Not only does this show that the EOF analysis reproduces the observed patterns better than the REOF loading pattern, but it also shows that the variability related to the PNA is split between the first two leading modes. There must therefore be some mixing between EOFs which would allow this to occur. Examining the leading eigenvalues from the EOF analysis, we note that the first two EOFs are just barely separated according to North et al.'s (1982) rule of thumb, meaning that these EOFs are only separated by approximately one standard deviation (i.e. the confidence interval of ~68 % for the two modes are just barely separated). This does not preclude the possibility of mixing between modes (Cheng et al. 1995). The fact that both the first and second EOFs share aspects of the PNA reinforce this. This lack of separation seems to indicate that the PNA, as a distinct low-frequency pattern of variability, is not stationary either in terms of it spatial extent nor its temporal variability, and tends to mix with the NAO related variability during the spring and early summer.

The first EOF mode resembles the Aleutian low-Icelandic low seesaw pattern in terms of its structure and relationship to both the PNA and NAO (Fig. 8a) (Honda and Nakamura 2001; Honda et al. 2007). From the first EOF we note that the North Atlantic and North Pacific pressure tend to covary in opposing signs. This indicates that the PNA and NAO may not be distinct modes of variability during these times when their indices are correlated. Both teleconnection patterns project onto this Aleutian low-Icelandic low seesaw pattern, which appears as the first EOF. Locally, in the Pacific and Atlantic basins, this pattern resembles the PNA and NAO, respectively, which explains the relationship between their indices. Each of the REOF loading patterns locally overlaps with this mode of variability, thus producing temporally correlated indices. Furthermore, given that the PNA's temporal variability can be equally explained by two modes of variability which are poorly separated, and the more important of these two modes is also related to the NAO, it is clear that the PNA and NAO are neither distinct, nor separable modes of variability.

5 Winters of 1985–2005

During the winters of 1985–2005 there is again statistically significant anti-correlation between the PNA and

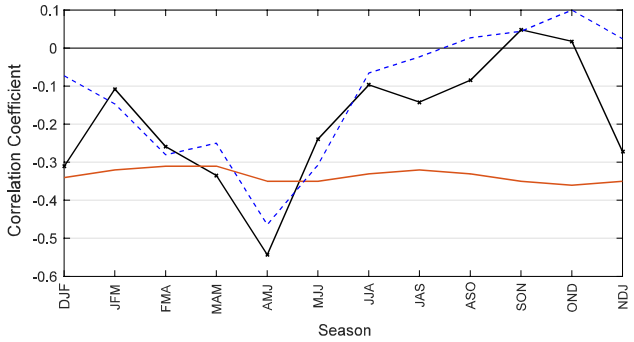

Fig. 9 The correlation between the PNA and NAO indices for every three-month season taken when the Nino-3.4 index is within 0.75 standard deviations of its mean. Values below the *red line* pass the 95 % significance level

NAO indices (Fig. 4). This feature of the correlation plot is statistically significant for varying window lengths of 15–25 years, with the maximum for a 21-year window width. This brief window indicates that the relationship between the teleconnection patterns at this time may be linked to some other decadal (or pseudo-decadal) process.

As in the last section there appears to be a slight disconnect between the tropical Pacific SST, given by the Nino-3.4 index, and the Northern Hemisphere geopotential height field. Here the correlation between the PNA and this region of SST is just below the 95 % significance level (correlation of 0.40); however, given the relatively large correlation and the short time period examined, it is unlikely that this slight disconnect is the only (or leading) cause of the anti-correlation between the PNA and NAO. However, for non-ENSO years, defined as those when the Nino-3.4 index amplitude is less than 0.75 standard deviations, the correlation between the PNA and NAO indices becomes greater. The correlation between these two indices increases from −0.07 in the complete winter record to −0.31 (not passing the 95 % significance level) in non-ENSO years (Fig. 9). This is also the case in the majority of the other seasons. When ENSO is weak, regardless of the season, the correlation between the PNA and NAO becomes more strongly negative. This implies that the relationship between the PNA and NAO tends to be strengthened in the absence of tropical forcing.

Even given this lack of concrete mechanism, there is good consistency between the spring relationship and the relationship during this winter period; in both cases there appears to be a lack of separation between the PNA and NAO patterns, as defined by the EOFs of the geopotential height field. The first EOF takes on an annular pattern with aspects of both the NAO and PNA embedded within it (Fig. 10a). It has a strong centre in the Northeast Pacific,

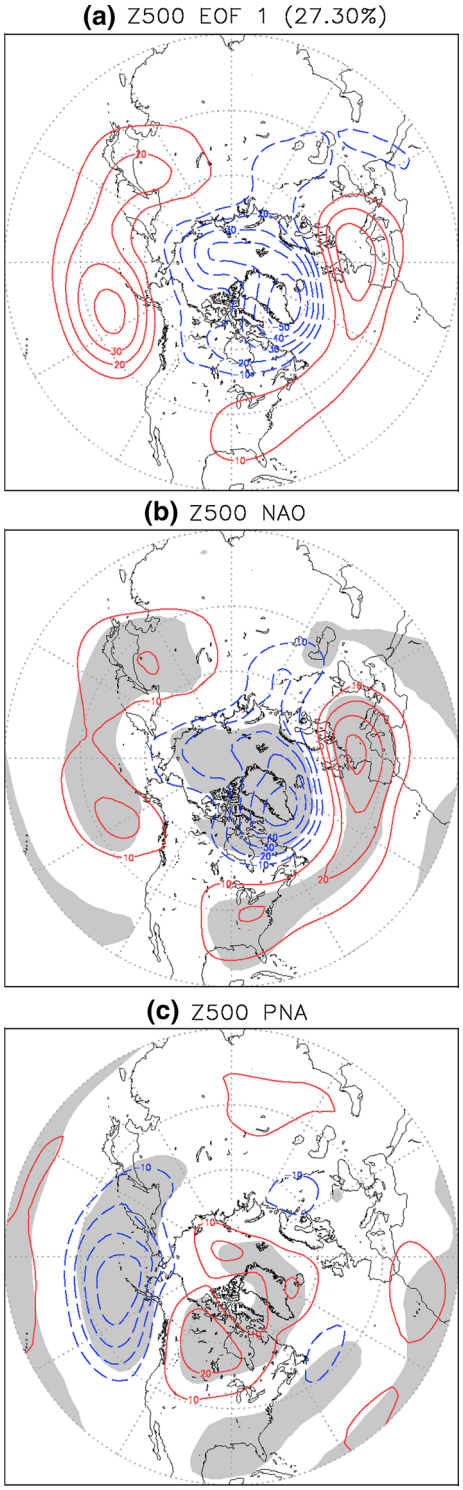

Fig. 10 **a** First EOF of 1985–2005 DJF 500 hPa geopotential height. *Bracketed value* is the variance explained by the mode. **b**, **c** are the regressions of the NAO and PNA, respectively, for this same time period. Values correspond to a change of one standard deviation of the respective time series. Contour interval is 10 m. *Grey shaded* areas pass the 95 % significance level

Table 3 Temporal correlation between the 1985–2005 DJF PNA and NAO, and the first two PCs of 500 hPa geopotential height

DJF	PC1	PC2
PNA	−0.7	0.34
NAO	0.96	−0.03

The bold values denote 95 % significance, while underlined values denote 99 % significance

Table 4 Patterns correlation between the PNA and NAO 1985–2005 DJF regression patterns, and the loading patterns used to derive their indices, as well as the first and second EOF patterns

DJF	Loading	EOF 1	EOF 2
PNA Regression	0.69	−0.66	**0.34**
NAO Regression	−0.77	0.96	0.19

The bold values denote 95 % significance, while underlined values denote 99 % significance

and the Arctic centre extends into Northwestern Canada. At this time the NAO closely resembles its typical configuration and the first EOF at this time (Fig. 10b), hence its high correlation with the first PC (Table 3). The surprising features lie within the PNA pattern (Fig. 10c), which has its North American centre, which normally lies along the West coast of the continent, shifted Northeast to the Canadian Prairies, and extends northward to cover Greenland. The pressure centre over Florida is also shifted northeast into the Atlantic Ocean off the coast of Newfoundland. These two spatial anomalies give a pattern which locally resemble the NAO. Like the spring case, the PNA does not appear in the EOF analysis as a separate mode of variability. The second EOF (not shown) has a wavenumber four pattern which projects onto the PNA pattern due to two of its centres lying over the Aleutian Islands, and Florida. However, despite this similarity, the PNA time series still varies more strongly with that of the first EOF (Table 3).

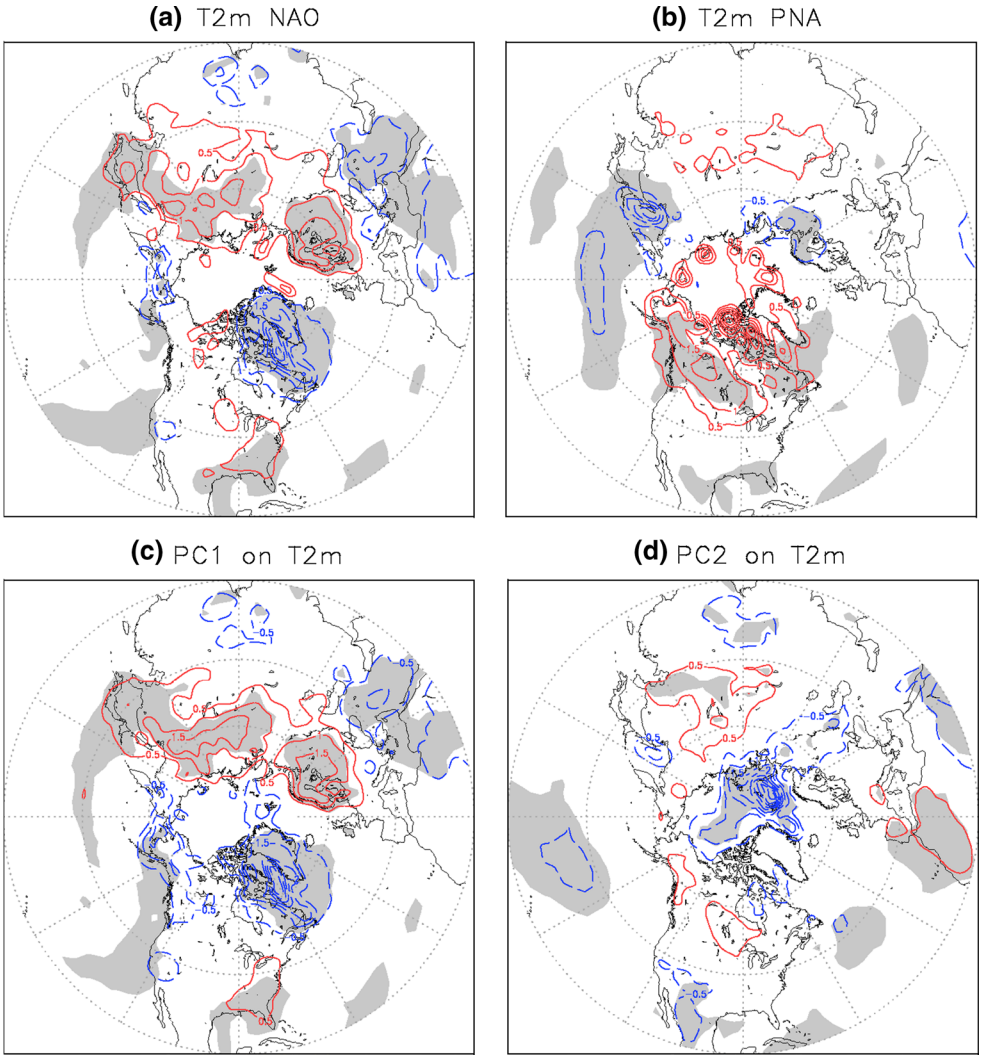

Fig. 11 Regression of the 1985–2005 winter **a** NAO and **b** PNA indices onto 2 m air temperature. **c**, **d** are the temperature fields associated with the first and second PCs, respectively. Contour interval is 0.5 °C. *Grey shading* denote areas passing the 95 % significance level

Examining the pattern correlations we obtain similar results to those presented in the previous section (Table 4). The PNA pattern is statistically related to the first two EOF patterns; however, like the NAO it is more strongly related to the first mode. The weak connection between the PNA and the second EOF can be attributed to its weak connection to ENSO. Here the Nino-3.4 index is strongly correlated with this second EOF mode (temporal correlation of 0.58, passing the 99 % significance level). Moreover, its regression pattern (not shown) strongly resembles the second EOF as well, with a pattern correlation of 0.76 (>99 % significance). This provides some evidence for the separation of the ENSO-forced PNA-like mode, and the PNA as an internal mode of variability (e.g. Straus and Shukla 2000, 2002). The internal portion of the PNA variability seems to be mixed with that of the NAO, in the first EOF, while the ENSO-forced variability is contained within the second mode. The PNA regression pattern is then nearly equally related to the first EOF as it is to the loading pattern used to define the index. This again shows that the PNA and NAO related variability are not separable. Finally, not only is the PNA's temporal variability much more strongly coupled to the first EOF mode, the pattern of temperature associated with the PNA index more closely resembles the pattern associated with the first PC (Fig. 11). This is again similar to the results for the spring.

6 Discussion and conclusion

The PNA and NAO indices, as obtained through a rotated EOF analysis using all four seasons, display a statistically significant anti-correlation during the spring and early summer over the entire time period available in the reanalysis dataset. During this season the PNA and NAO do not appear as distinct modes of variability, they instead appear to be part of a single mode of variability which takes on a pseudo-zonally symmetric annular pattern. During the winter months, the PNA and NAO appear as two distinct low frequency anomaly patterns, with temporally independent indices (Figs. 6, 2). This is not surprising, as the REOF analysis gives more weight to the winter data. The exception to this is a brief period of two decades for which there is a statistically significant anti-correlation between the two teleconnection patterns. This winter connection has been linked to the Pacific Decadal Oscillation, where the relationship between the tropical Pacific SST and Northern Hemisphere geopotential heights is weakened when the PDO shifts to its positive phase (Zhao and Moore 2009). During the spring and early summer the tropical Pacific SST exerts only a marginal effect on the Northern Hemisphere geopotential height field; whereas during the winters of 1985-2005 the influence of the tropical Pacific SST is independent of both internal teleconnection patterns.

It is this type of disconnect between the tropical Pacific SSTs and the geopotential height field that occurs annually during the spring and early summer. When this disconnect occurs, whether annually in the spring, or periodically during other seasons, the strength of the relationship between the tropical Pacific SST and the PNA also diminishes. This results in the PNA's internal variability, and its forced variability (related to El-Nino) to become separated. At times when the PNA and NAO are temporally correlated, they are not two separate patterns as in the majority of winters, but rather a sort of aggregate pattern which contains features of both teleconnections. During these periods of time, defining the PNA and NAO indices based upon an loading patterns from an REOF analysis yields two related time series which are not independent from one another, and do not represent the standing oscillations which underlie the climate variability. Their resulting spatial structures represent two spatially overlapping projections of a single pattern of variability, as can be seen from the regression of their indices onto the geopotential height field (Fig. 7). The difference in the regression patterns of each of the teleconnections can be explained by the difference in the loading patterns used to define the indices.

Given that the teleconnection indices are computed by projection onto loading patterns, which take into account the anomaly field over the entire hemisphere, a natural solution would be to then examine the station based indices of these two teleconnection patterns. In this way we can isolate locations we know covary, and ignore the rest of the data map. We therefore computed the PNA index using the definition which Wallace and Gutzler (1981) put forth based on normalized 500 hPa geopotential height anomalies. For the NAO index we use the normalized sea-level pressure difference between points near Azores, Portugal, and Reykjavík, Iceland. These two new indices are again not significantly correlated during the winter months (corr $= -0.18$), and are statistically significantly correlated during AMJ (corr $= -0.40$, >99 % significance). The relationship found during the winters of 1985–2005 is also present, and statistically significant (corr $= -0.55$, >99 % significance). Moreover, the regression patterns associated with the station indices (not shown) are nearly identical to those associated with the indices derived by projection onto REOF loading patterns. This lends confidence to the conclusion drawn above, in that the connection is not likely an artifact of the method of computation, but rather a robust relationship whereby the remote locations associated with each the PNA and NAO, which do not generally covary, do so during the spring and early summer, and during the winters of certain decades.

These results imply that when the PNA and NAO indices are found to be correlated, we cannot treat them as separate modes of variability, but should rather examine

the corresponding EOF mode. Otherwise we force the time series to take into account locations which may not, at the time, covary, and thus lead to spurious results when examining the fields associated with these time series. Therefore care must be taken when deriving teleconnection indices from archetypal loading patterns or stations.

Acknowledgments The authors would like to thank Dr. Jacques Derome for helpful comments on an early version of the manuscript. This research was made possible by a Natural Sciences and Engineering Research Council of Canada (NSERC) Discovery Grant to the second author. We thank two anonymous reviewers whose comments helped to improve our paper.

References

Barnston AG, Livezey RE (1987) Classification, seasonality and persistence of low-frequency atmospheric circulation patterns. Mon Weather Rev 115(6):1083–1126

Blackmon ML, Lee Y-H, Wallace JM (1984) Horizontal structure of 500 mb height fluctuations with long, intermediate and short time scales. J Atmos Sci 41(6):961–980

Cheng X, Nitsche G, Wallace JM (1995) Robustness of low-frequency circulation patterns derived from EOF and rotated EOF analyses. J Clim 8:1709–1713

Hoerling MP, Kumar A, Xu T (2001) Robustness of the nonlinear climate response to ENSO's extreme phases. J Clim 14(6):1277–1293

Honda M, Nakamura H (2001) Interannual seesaw between the Aleutian and Icelandic lows. Part II: its significance in the interannual variability over the wintertime Northern hemisphere. J Clim 14:4512–4529

Honda M, Nakamura H, Ukita J, Kousaka I, Takeuchi K (2001) Interannual seesaw between the Aleutian and Icelandic lows. Part I: seasonal dependence and life cycle. J Clim 14:1029–1042

Honda M, Yamane S, Nakamura H (2007) Inter-basin link between the North Pacific and North Atlantic in the upper tropospheric circulation: its dominance and seasonal dependence. J Meteorol Soc Jpn 85(6):899–908

Horel JD (1981) A rotated principal component analysis of the interannual variability of the northern hemisphere 500 mb geopotential height field. Mon Weather Rev 109:2080–2092

Hurrell JW, van Loon H (1997) Decadal variations in climate associated with the North Atlantic Oscillation. Clim Change 36:301–326

Hurrell JW, Kushnir Y, Ottersen G, Visbeck M (2003) An overview of the North Atlantic Oscillation. In: Hurrell JW, Kushnir Y, Ottersen G, Visbeck M (eds) The North Atlantic Oscillation: climatic significance and environmental impact. American Geophysical Union, Washington, pp 1–35

Johnson NC, Feldstein SB (2010) The continuum of North Pacific sea level pressure patterns: intraseasonal, interannual, and interdecadal variability. J Clim 23(4):851–867

Kalnay E, Kanamitsu M, Kistler R, Collins W, Deaven D, Gandin L, Iredell M, Saha S, White G, Woollen J, Zhu Y, Leetmaa A, Reynolds R, Chelliah M, Ebisuzaki W, Higgins W, Janowiak J, Mo KC, Ropelewski C, Wang J, Jenne R, Joseph D (1996) The NCEP/NCAR 40-year reanalysis project. B Am Meteorol Soc 77(3):437–471

Latif M, Barnett TP, Cane MA, Flugel M, Graham NE, Von Storch H, Xu J-S, Zebiak SE (1994) A review of ENSO prediction studies. Clim Dyn 9(4–5):167–179

Lin H, Derome J (2004) Nonlinearity of the extratropical response to tropical forcing. J Clim 17(13):2597–2608

Lin H, Brunet G, Derome J (2009) An observed connection between the North Atlantic Oscillation and the Madden–Julian Oscillation. J Clim 22(2):364–380

Mo R, Fyfe J, Derome J (1998) Phase-locked and asymmetric correlations of the wintertime atmospheric patterns with the ENSO. Atmos Ocean 36(3):213–239

North G, Bell T, Cahalan R, Moeng F (1982) Sampling errors in the estimation of empirical orthogonal functions. Mon Weather Rev 110:699–706

Peng P, Kumar A (2005) A Large ensemble analysis of the influence of tropical SSTs on seasonal atmospheric variability. J Clim 18(7):1068–1085

Pinto JG, Reyers M, Ulbrich U (2010) The variable link between PNA and NAO in observations and in multi-century CGCM simulations. Clim Dyn 36(1–2):337–354

Pozo-Vázquez D, Esteban-Parra MJ, Rodrigo FS, Castro-Díez Y (2001) The association between ENSO and winter atmospheric circulation and temperature in the North Atlantic region. J Clim 14(16):3408–3420

Pozo-Vázquez D, Gámiz-Fortis SR, Tovar-Pescador J, Esteban-Parra MJ, Castro-DÍez Y (2005) El Nino-Southern Oscillation events and associated European winter precipitation anomalies. Int J Climatol 25(1):17–31

Song J, Li C, Zhou W, Pan J (2009) The linkage between the Pacific-North American teleconnection pattern and the North Atlantic Oscillation. Adv Atmos Sci 26(2):229–239

Straus DM, Shukla J (2000) Distinguishing between the SST-forced variability and internal variability in mid latitudes: analysis of observations and GCM simulations. Q J R Meteorol Soc 126(567):2323–2350

Straus DM, Shukla J (2002) Does ENSO force the PNA? J Clim 15(17):2340–2358

Thompson DW, Wallace JM (1998) The Arctic Oscillation signature in the wintertime geopotential height and temperature fields. Geophys Res Lett 25(9):1297–1300

Van Loon H, Rogers JC (1978) The seesaw in winter temperatures between Greenland and Northern Europe. Part I: general description. Mon Weather Rev 106(3):296–310

Wallace JM (2000) North Atlantic Oscillation/annular mode: two paradigms—one phenomenon. Q J R Meteorol Soc 126:791–805

Wallace JM, Gutzler DS (1981) Teleconnections in the geopotential height field during the Northern hemisphere winter. Mon Weather Rev 109(4):784–812

Zhao H, Moore GWK (2009) Temporal variability in the expression of the Arctic Oscillation in the North Pacific. J Clim 22(11):3110–3126